# Chapter 16
# Ultrasonic Nonlinear Guided Waves and Applications to Structural Health Monitoring

**Claudio Nucera and Francesco Lanza di Scalea**

**Abstract** Research efforts on nonlinear guided wave propagation have increased dramatically in the last few decades because of the large sensitivity of nonlinear waves to structural condition (defects, quasi-static loads, instability conditions, etc.. . .). However, the mathematical framework governing the nonlinear guided wave phenomena becomes extremely challenging in the case of waveguides that are complex in either materials (damping, anisotropy, heterogeneous, etc.. . .) or geometry (multilayers, geometric periodicity, etc.. . .). The present work develops predictions of nonlinear second-harmonic generation in complex waveguides by extending the classical Semi-Analytical Finite Element formulation to the nonlinear regime, and implementing it into a highly flexible, yet very powerful, commercial Finite Element code. Results are presented for the following cases: a railroad track, a viscoelastic plate, a composite quasi-isotropic laminate, and a reinforced concrete slab. In these cases, favorable combinations of primary wave modes and resonant double-harmonic nonlinear wave modes are identified. Knowledge of such combinations is important to the implementation of structural monitoring systems for these structures based on higher-harmonic wave generation. The presentation will also present a specific application of nonlinear guided waves for the monitoring of thermal stresses in rail tracks to prevent buckling.

**Keywords** Nonlinear ultrasonic guided waves • Higher-harmonics • Semi-analytical finite element • Internal resonance • Dispersion

## 16.1 Introduction

Traditionally the structural monitoring via ultrasounds has been accomplished measuring "linear" parameters of the waves (amplitude, speed, phase shifts) to infer salient features of the inspected structure. However, it is well documented [6] that "nonlinear" parameters are, in general, much more sensitive to structural conditions than their linear counterparts. Furthermore the use of nonlinear guided waves is extremely attractive because guided waves combine the mentioned high sensitivity typical of nonlinear parameters with large inspection ranges [3, 5, 14]. The aforementioned complexity of the mathematical framework governing nonlinear guided wave propagation limited most of the previous works on elastic waves to the linear elastic regime with the assumption of infinitesimal deformations.

However, different mechanisms (increase in wave amplitude, finite deformations, nonlinear strain energy potentials) can give rise to nonlinear effects that eventually become of primary importance. Hence the governing equations need to be modified accordingly: cubic (and possibly higher-order) terms must be included in the elastic energy density expression [9, 16]. Among the manifestations of the nonlinear behavior, higher harmonic generation is considered in particular. In this scenario, an initially sinusoidal stress wave of a given frequency distorts as it propagates, and energy is transferred from the fundamental frequency, $\omega$, to the higher harmonics, $2\omega$, $3\omega$ and so on. For a practical use, this nonlinearity can be quantified via an ultrasonic nonlinear parameter, $\beta$, well documented in literature [3].

While several investigations pertaining to nonlinear effect in solids and second harmonic generation were reported in the past [7, 8], most of them were limited in their applicability to structures with simple geometries (plates, rods, shells) where analytical solutions for the primary (linear) wave field are available in literature. In the present work the propagation of

C. Nucera (✉) • F.L. di Scalea
Department of Structural Engineering, University of California, San Diego, 9500 Gilman Drive, M.C. 0085, La Jolla, CA 92093-0085, USA
e-mail: cnucera@ucsd.edu; flanza@ucsd.edu

M. Rossi et al. (eds.), *Residual Stress, Thermomechanics & Infrared Imaging, Hybrid Techniques and Inverse Problems, Volume 8*, Conference Proceedings of the Society for Experimental Mechanics Series, DOI 10.1007/978-3-319-00876-9_16,

waves in nonlinear solid waveguides with complex geometrical and material properties is investigated theoretically and numerically. For the solution of the nonlinear boundary value problem, perturbation theory and modal expansion are used [7].

A numerical algorithm is introduced in order to efficiently predict and explore the nonlinear wave propagation phenomena in structural waveguides of different complexity. After a brief description of the theoretical background, three case-studies have been analyzed, namely a railroad track, a composite quasi-isotropic laminate, and a reinforced concrete slab. Favorable combinations of primary and resonant secondary modes (nonlinear resonance conditions) were successfully identified for these complex waveguides. The knowledge of these nonlinear resonance conditions is of primary importance for the actual implementation of structural diagnostic systems based on nonlinear ultrasonic guided waves features.

## 16.2 Waves in Nonlinear Elastic Regime: Internal Resonance

In presence of finite deformations, large amplitude waves, nonlinear strain energy potentials and similar nonlinear mechanisms, the generalized Hooke's Law no longer applies and must be replaced by a proper nonlinear constitutive law. Assuming that the body is homogeneous, isotropic and hyperelastic, it possesses a strain energy density $\boldsymbol{\varepsilon}$ that is an analytic function of the Green-Lagrange Strain Tensor $\boldsymbol{E}$ such that the Second Piola-Kirchoff Stress Tensor $\boldsymbol{S}$ can be expressed as:

$$S_{ij} = \rho_0 \frac{\partial \varepsilon}{\partial E_{ij}} \tag{16.1}$$

where $\boldsymbol{\rho_0}$ is the initial density. It is known that in this scenario the strain energy can be expressed as:

$$\varepsilon = \frac{1}{2}\lambda {I_1}^2 + \mu I_2 + \frac{1}{3} C {I_1}^3 + B I_1 I_2 + \frac{1}{3} A I_3 + O\left({E_{ij}}^4\right) \tag{16.2}$$

where $\boldsymbol{I_1 = E_{ii}}$, $\boldsymbol{I_2 = E_{ij}E_{ji}}$, $\boldsymbol{I_3 = E_{ij}E_{jk}E_{ki}}$, $\boldsymbol{\lambda}$ and $\boldsymbol{\mu}$ are the Lamé elastic constants and $\boldsymbol{A}$, $\boldsymbol{B}$ and $\boldsymbol{C}$ are the Landau-Lifshitz third-order elastic constants [10]. In Eq. 16.2 first order material nonlinearity was introduced. By substituting Eq. 16.2 into Eq. 16.1 and keeping up to second-order terms in $\boldsymbol{E_{ij}}$ we obtain the nonlinear stress–strain relation

$$S_{ij} = \lambda E_{kk}\delta_{ij} + 2\mu E_{ij} + \delta_{ij}(C E_{kk}E_{ll} + B E_{kl}E_{lk}) + 2B E_{kk}E_{ij} + A E_{jk}E_{ki} \tag{16.3}$$

Using Eq. 16.3 inside the general momentum equation the Nonlinear Boundary Value Problem governing the propagation of nonlinear elastic waves in isotropic, homogeneous and hyperelastic waveguides can be formulated in vector form as:

$$(\lambda + 2\mu)\nabla(\nabla \cdot u) - \mu \nabla \times (\nabla \times u) + f = \rho_0 \frac{\partial^2 u}{\partial t^2} \tag{16.4}$$

$$S^L(u) \cdot n_r = -\bar{S}(u) \cdot n_r \qquad \text{on} \qquad \Gamma \tag{16.5}$$

where $\boldsymbol{u}$ is the particle displacement vector, $\boldsymbol{\rho_0}$, $\boldsymbol{\lambda}$ and $\boldsymbol{\mu}$ are the defined above, $\boldsymbol{f}$ is the nonlinear term acting as a body force, $\boldsymbol{n_r}$ is the unit vector normal to the surface of the waveguide $\boldsymbol{\Gamma}$ and $\boldsymbol{S_L}$ and $\bar{S}$ are the linear and nonlinear parts of the second Piola-Kirchoff stress tensor, respectively. The nonlinear boundary value problem in Eqs. 16.4 and 16.5 is solved in the following using perturbation theory, which is based on writing the solution as sum of two terms, namely $\boldsymbol{u = u^{(1)} + u^{(2)}}$, where $\boldsymbol{u^{(1)}}$ is the primary solution and $\boldsymbol{u^{(2)}}$ is the secondary solution due to nonlinearity, this assumed to be small compared to $\boldsymbol{u^{(1)}}$ (*perturbation condition*). Using this condition the original nonlinear boundary value problem is divided into two linear boundary value problems, namely the first-order and second-order approximations. Following [1] and [7], if $\boldsymbol{\omega}$ is the primary frequency that we suppose to convey into the system via a monochromatic wave, the first order nonlinear solution is calculated through modal expansion using the existing propagating guided modes $\boldsymbol{2\omega}$ as:

$$v(x, y, z, t) = \frac{1}{2} \sum_{m=1}^{\infty} A_m(z) v_m(x, y) e^{-i2\omega t} + c.c. \tag{16.6}$$

where ***c.c.*** denotes complex conjugates, $\boldsymbol{v_m}$ is the particle velocity vector referred to the $m$th mode at $2\boldsymbol{\omega}$ and $\boldsymbol{A_m}$ is the higher order modal amplitude given by

$$A_m(z) = \bar{A}_m(z)e^{i(2kz)} - \bar{A}_m(0)e^{ik_n{}^*z} \tag{16.7}$$

All the details regarding the calculation of the modal amplitudes can be found in [7]. At this stage it is important to emphasize how the internal resonance mechanism, which in turn produces a cumulative nonlinear response, relies on the simultaneous occurrence of two conditions, namely:

1. Phase Matching: $k_n{}^* = 2k$
2. Non-zero power transfer from primary to secondary wave: $f_n{}^{surf} + f_n{}^{vol} \neq 0$

## 16.3 CO.NO.SAFE Algorithm

The Semi-Analytical Finite Element formulation (*S.A.F.E.*) in its linear fashion has been extensively discussed in the past highlighting its great potential in efficiently calculating the dispersion properties of waveguide-like structures. These properties are crucial for the implementation of any SHM system based on the use of ultrasonic guided waves. Concerning the detail of the classical *SAFE* formulation, the interested reader is referred to [2]. In the present work the classical linear formulation is extended to the nonlinear regime according to the theory discussed in the previous section. The resultant **No**nlinear **S.A.F.E.** formulation is implemented into **CO**MSOL commercial code (***CO.NO.SAFE***). In this way the full power of existing libraries and routines of the commercial code is exploited and the internal resonance conditions of several structural waveguides of different complexity can be studied in a straightforward manner via user-friendly interfaces.

Furthermore, since all the nonlinear parameters involve gradients of the displacement field up to the third order [7], high-order finite elements (at least cubic) need to be used in order to obtain meaningful results; this implement is not always trivial for general non-commercial SAFE algorithm. Starting from the nonlinear boundary value problem described in Eqs. 16.4 and 16.5, the displacement field is approximated in the cross-section of the waveguide and is enforced to be harmonic in time and along the direction of wave propagation. For the generic $e$th element this reads:

$$u^e = N^e U^e e^{i(kz-\omega t)} \tag{16.8}$$

where $\boldsymbol{N^e} = \boldsymbol{N^e(x,y)}$ is the matrix of shape functions and $\boldsymbol{U^e}$ is the nodal displacement vector for the $e$th element. Assuming this displacement field in (4–5) is the only trivial modification that needs to be done in the original FEM formulation. The original quadratic eigenvalue problem is linearized doubling the space dimension [2]. The nonlinear boundary value problem has been implemented in COMSOL using the general PDE solver engine. The COMSOL formalism for the boundary value problem with Neumann B.C. (which corresponds to the guided wave propagation since a stress-free B.C. needs to be applied) is:

$$\nabla \cdot (c\nabla U + \alpha U - \gamma) - \beta \cdot \nabla U - aU + \lambda d_a U = 0 \tag{16.9}$$

$$n \cdot (c\nabla U + \alpha U) + qU = 0 \tag{16.10}$$

where $\boldsymbol{U}$ represents the set of dependent variables to be determined and all the remaining quantities are matrix coefficients admitting complex values, which is essential for viscoelastic materials. The nonlinear part of the algorithm has been coded in MATLAB and connected to COMSOL using the *LiveLink* package.

In this way, once the dispersion properties are obtained, several possible combinations of potential resonant modes are selected and analyzed. Resonant modes are identified making use of the phase-matching and non–zero power transfer conditions discussed before. The possibility to assess internal resonance conditions for complex solid waveguides is crucial for the efficiency of a given SHM inspection approach. In fact, once a resonant combination of modes is identified, nonlinear response becomes cumulative, namely the amplitude of the second harmonic grows with distance [7]. In this way the efficiency of the given nonlinear technique is dramatically maximized.

## 16.4 Applications

### *16.4.1 Railroad Track*

The widely used 136 lb RE railroad track was considered as first case-study. Due to the complex geometry of the cross section, dispersion curves and, consequently, higher harmonic generation conditions cannot be calculated analytically. The material properties considered are given in Table 16.1. The Landau-Lifshitz third-order elastic constants are detailed in [15].

The complexity of the guided wave propagation for this particular waveguide is evident considering the abundance of possible propagative modes present (Fig. 16.1a) and the complexity of the phase-velocity dispersion curves (Fig. 16.1b), especially at higher frequencies.

A flexural vertical mode was selected as primary excitation at 80 kHz. The results of the CO.NO.SAFE analysis disclosed the presence of some synchronous secondary modes at 160 kHz with one in particular (slightly different flexural vertical type) able to produce internal resonance. Figure 16.2a, b display the selected modes, while Fig. 16.2c spotlights the very high value of modal amplitude related to the only secondary resonant mode; small amplitude values associated to the other

**Table 16.1** Material properties assumed for the railroad track analysis

| $\rho$ [kg/m$^3$] | $\lambda$ [GPa] | $\mu$ [GPa] | $A$ [GPa] | $B$ [GPa] | $C$ [GPa] |
|---|---|---|---|---|---|
| 7,932 | 116.25 | 82.754 | −340 | −646.667 | −16.667 |

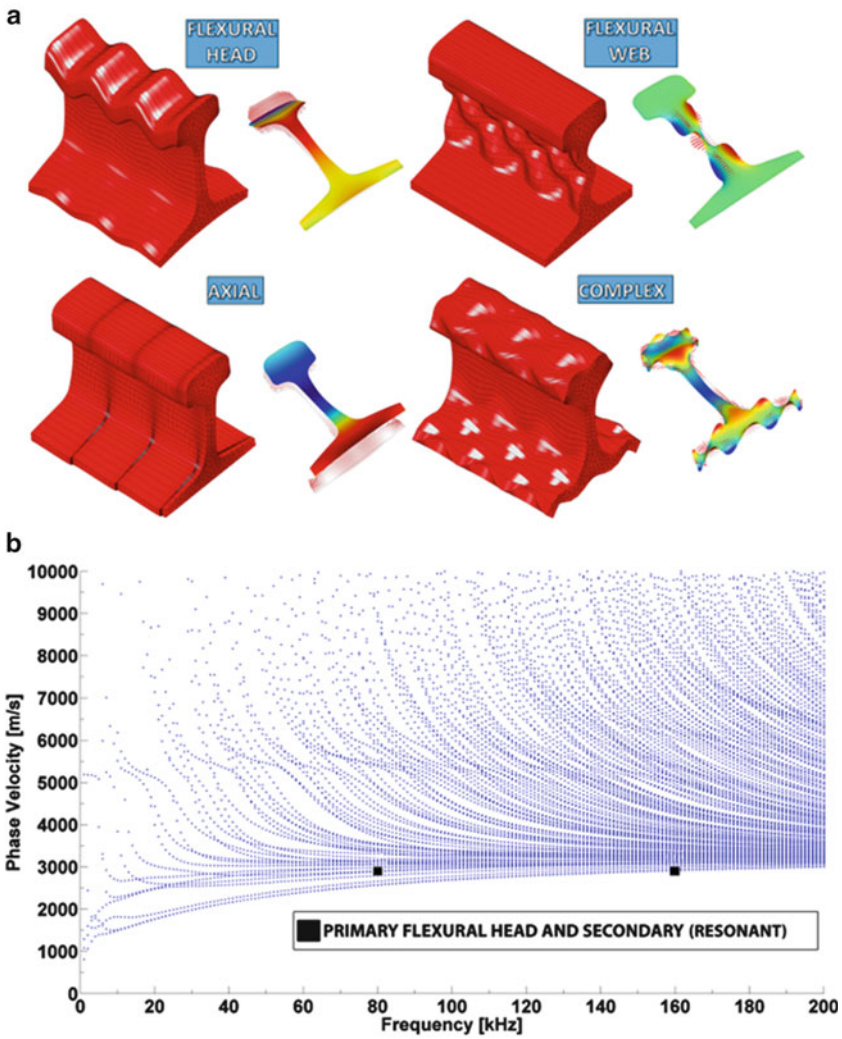


**Fig. 16.1** (**a**) Exemplary propagative modes in the rail. (**b**) Phase-velocity dispersion curves in the (0–200) kHz frequency range with primary and secondary modes highlighted

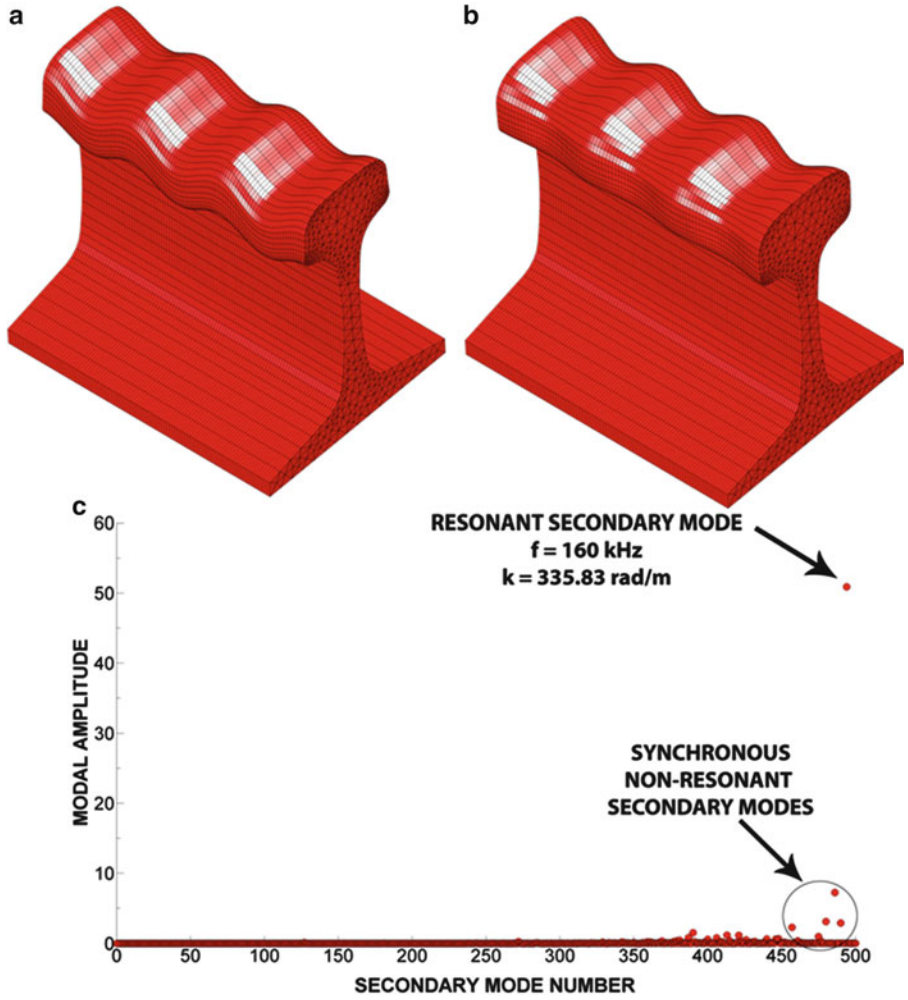


**Fig. 16.2** (**a**) Selected primary mode at 80 kHz. (**b**) Resonant secondary mode at 160 kHz. (**c**) Modal amplitude plot for secondary propagative modes

synchronous modes, for which power transfer is absent, are also shown in the same figure. The previous results point up a favorable combination of primary and secondary wave fields able to maximize the nonlinear response of the waveguide.

### *16.4.2 Anisotropic Elastic Composite Laminate*

A multi-layered composite laminate with unidirectional laminae in a quasi-isotropic layup was examined next. More specifically, the selected system consists of eight unidirectional T800/924 graphite-epoxy plies with a stacking sequence of $[\pm 45/0/90]_S$. Each layer has a thickness of 0.125 mm resulting in a total laminate thickness of 1 mm. The material properties for each single lamina in the principal directions of material symmetry are: $\rho = 1{,}500$ kg/m$^3$, $E_{11} = 161$ GPa, $E_{22} = 9.25$ GPa, $G_{12} = 6.0$ GPa, $\nu_{12} = 0.34$ and $\nu_{23} = 0.41$ [11]. The stiffness matrix for each lamina was rotated according to the angle between the fiber direction and the wave propagation direction [2]. In the following, wave propagation was assumed at 0° with respect to the fiber direction 1 (the extension to cases where this angle assumes different values is trivial). After all the matrices were rotated, the governing eigenvalue problem was solved as in the previous sections using the rotated stiffness matrices in the constitutive relations. Periodic Boundary Conditions (PBCs) were employed to gain computational efficiency [12]. The third-order elastic constants assumed for each lamina are: $A = 15$, $B = -33$ and $C = -14$ GPa [13]. The nonlinear post-processing was developed between 2.5 and 5.0 MHz. A complex primary mode

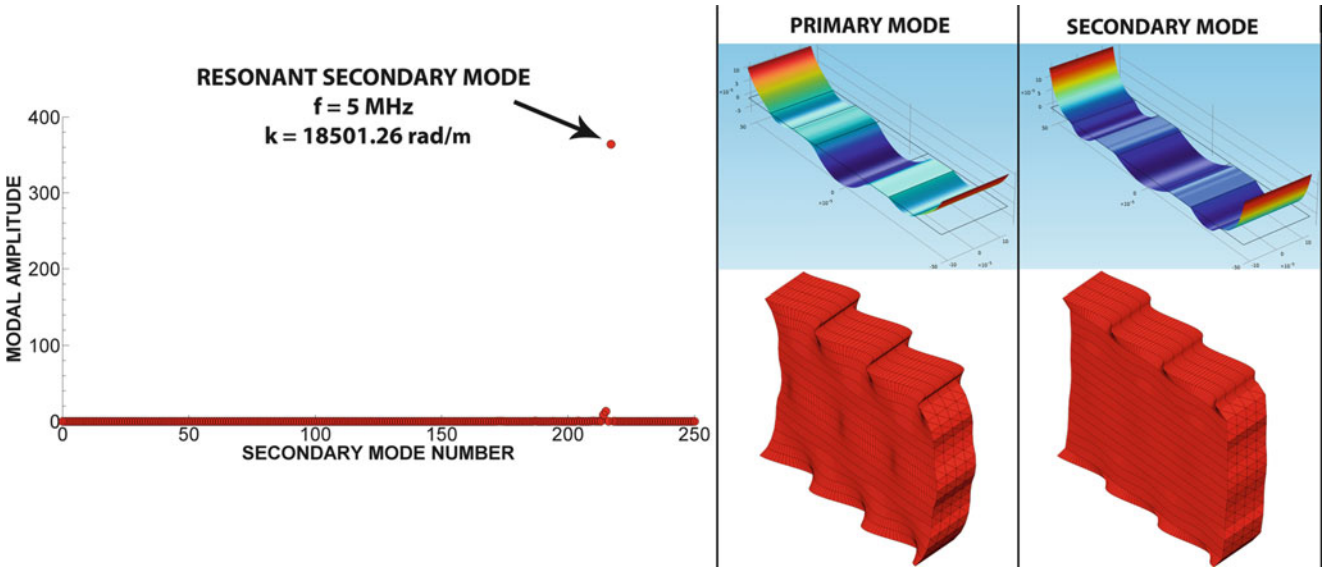


**Fig. 16.3** Modal amplitude plot for secondary propagative modes, along with contour plots and 3D views of the selected primary and secondary modes for the elastic composite laminate

combining attributes typical of axial and flexural horizontal modes was selected as input. One of the propagative modes at the double harmonic (5 MHz) was found able to produce internal resonance. The results, in terms of modal amplitude plots, are shown in Fig. 16.3 along with the primary and secondary modeshapes. It can be noted from Fig. 16.3 how drastic is the predominance of the only resonant mode in terms of modal amplitude, when compared to all the other propagative secondary modes existing at 5 MHz. Both primary and secondary modes concentrate the wave energy near the center of the waveguide; consequently, this combination appears appealing for the inspection of the laminate because of the expected reduced wave leakage into surrounding areas.

### *16.4.3 Reinforced Concrete Slab*

The complexity here arises from the coexistence of two domains with very different material properties. Previous studies have shown the influence of the reinforcement on the dispersion curves [12]. The present work analyzes the nonlinear features of the guided wave propagation for this particular heterogeneous system. Likewise the previous case PBCs are used to model the geometrical periodicity. The 2D periodic cell considered is 6 cm wide and 8 cm tall. The steel bars are assumed to be 1.6 cm in diameter (Fig. 16.4a). Material properties assumed for the concrete domain are: $\rho = 2{,}133$ kg/m$^3$, $C_{11} = 33.2$ GPa, $C_{66} = 11.8$ GPa [4]. For the steel bars, the following values were used: $\rho = 7{,}900$ kg/m$^3$, $C_{11} = 280$ GPa, $C_{66} = 80$ GPa [12]. The CO.NO.SAFE algorithm was used with 40 kHz as the primary frequency. The primary mode selected as input exhibits essentially a flexural horizontal displacement field.

The nonlinear results are presented in Fig. 16.4b. They reveal the presence of few asynchronous modes characterized by relatively large power transfer (modal amplitude values inside the circle) and only a single resonant secondary mode able to verify also the phase-matching condition. The nature of this identified advantageous combination of modes is represented in Fig. 16.4b.

## 16.5 Conclusions

The use of nonlinear guided waves is gaining increasing attention in the non-destructive evaluation and structural health monitoring communities. Proper application of nonlinear measurements requires a thorough understanding of the higher-harmonic generation phenomena that can be expected for the test waveguide. In the present work, the classical S.A.F.E. algorithm was extended to the nonlinear regime and implemented in a powerful multipurpose commercial FEM code

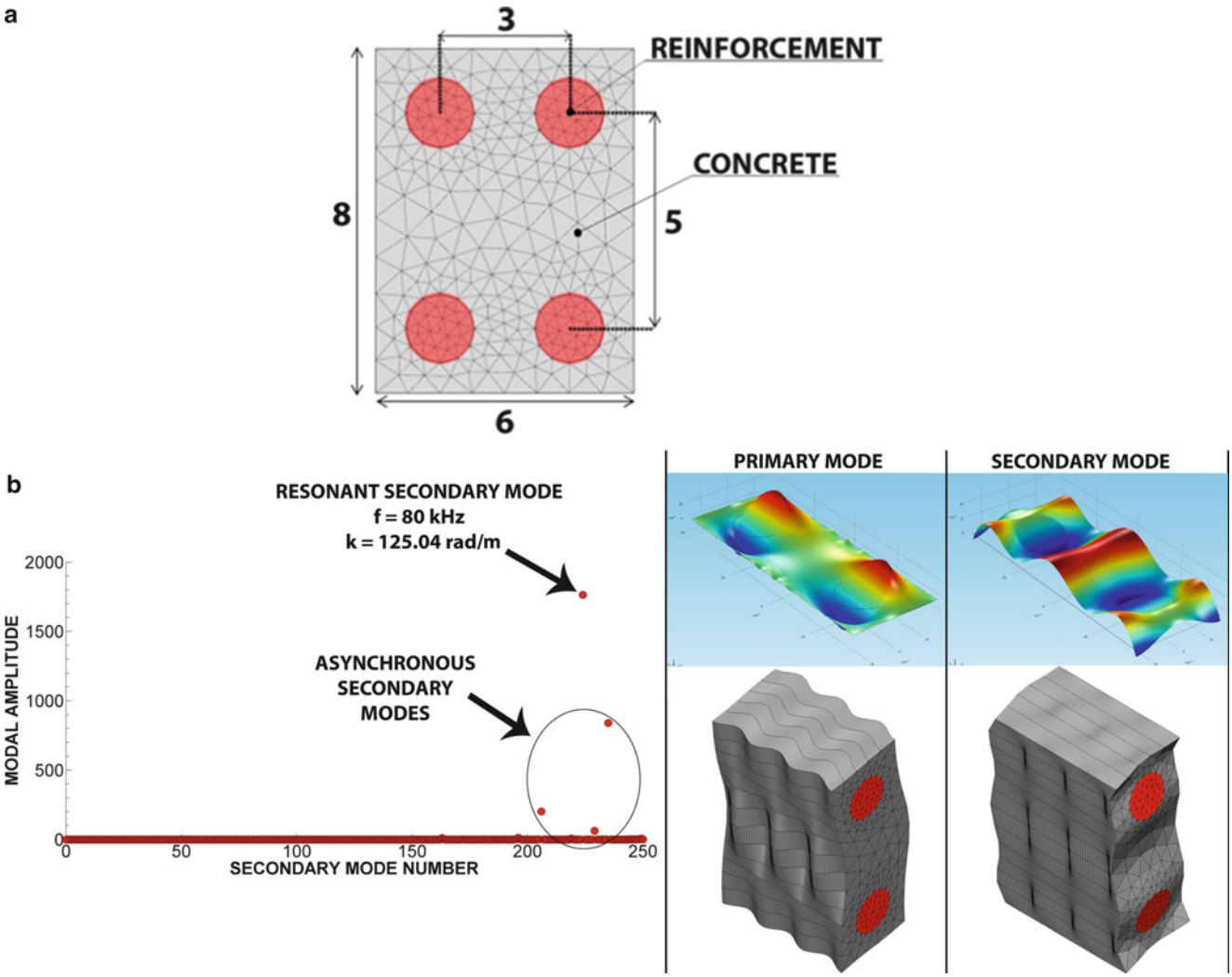


**Fig. 16.4** (**a**) Geometrical details and finite element mesh for the periodic cell representative of a 8 cm thick reinforced concrete slab (dimensions in cm). (**b**) Modal amplitude plot for secondary propagative modes along with contour plots and 3D views of the selected primary and secondary modes for the reinforced concrete slab

(COMSOL). The result is a new tool that opens new possibilities for the analysis of dispersion characteristics and, most importantly here, nonlinear internal resonance conditions, for a variety of complex structural waveguides that do not lend themselves to alternative analyses such as purely analytical solutions.

The specific "complex" cases that were examined include: complex geometry (railroad track), multilayered composite panels (8-ply quasi-isotropic laminate), and heterogeneous periodic systems (reinforced concrete slab). In all these cases, the proposed algorithm successfully identified appropriate combinations of resonant primary and secondary modes that exhibit the desired conditions of synchronicity and large cross-energy transfer. These properties can be exploited in an actual system aimed at monitoring the structural condition of the waveguide by nonlinear waves (detect defects, measure quasi-static loads or instability conditions, etc.).

## References

1. Auld BA (1990) Acoustic fields and waves in solids. Krieger, Malabar
2. Bartoli I, Marzani A, di Scalea FL, Viola E (2006) Modeling wave propagation in damped waveguides of arbitrary cross-section. J Sound Vib 295:685–707
3. Bermes C, Kim JY, Qu JM, Jacobs LJ (2007) Experimental characterization of material nonlinearity using lamb waves. Appl Phys Lett 90:0219011–0219013

4. Bouhadjera A (2004) Simulation of in-situ concrete conditions using a novel ultrasonic technique. In: Proceedings of 16th world conference on non-destructive resting, Montreal, Canada, 30 Aug–3 Sept 2004
5. Cawley P, Alleyne D (1996) The use of lamb waves for the long range inspection of large structures. Ultrasonics 34:287–290
6. Dace G, Thompson R, Rehbein D, Buck O (1991) Nonlinear acoustic, a technique to determine microstructural changes in material. Rev Prog Quant NDE 10B:1685–1692
7. de Lima WJN, Hamilton MF (2003) Finite-amplitude waves in isotropic elastic plates. J Sound Vib 265:819–839
8. Deng MX (2003) Analysis of second-harmonic generation of lamb modes using a modal analysis approach. J Appl Phys 94:4152–4159
9. Goldberg ZA (1960) Interaction of plane longitudinal and transverse elastic waves. Soviet Phys Acoust 6(3):306–310
10. Landau LD, Lifshitz EM (1959) Theory of elasticity. Wesley, London
11. Percival WJ, Birt EA (1997) A study of lamb wave propagation in carbon-fibre composites. Insight 39:728–735
12. Predoi MV, Castaings M, Hosten B, Bacon C (2007) Wave propagation along transversely periodic structures. J Acoust Soc Am 121:1935–1944
13. Prosser WH (1987) Ultrasonic characterization of the nonlinear elastic properties of unidirectional graphite/epoxy composites. NASA Contract Rep 4100:75–120
14. Rose JL (2002) Standing on the shoulders of giants: an example of guided wave inspection. Mater Eval 60:53–59
15. Sekoyan SS, Eremeev AE (1966) Measurement of the third-order elasticity constants for steel by the ultrasonic method. Meas Tech 0543–1972:888–893
16. Zarembo LK, Krasil'nikov VA (1971) Nonlinear phenomena in the propagation of elastic waves in solids. Soviet Phys USPEKHI 13:778–797